Autophagy 9:1, 5–19; January 2013; © 2013 Landes Bioscience

Recombinant protein rVP1 upregulates BECN1-independent autophagy, MAPK1/3 phosphorylation and MMP9 activity via WIPI1/WIPI2 to promote macrophage migration

Chiao-Chun Liao,[1,2] Ming-Yi Ho,[2] Shu-Mei Liang[1,2,3,*] and Chi-Ming Liang[1,2,4,*]

[1]Graduate Institute of Life Sciences; National Defense Medical Center; Taipei, Taiwan; [2]Genomics Research Center; Academia Sinica; Taipei, Taiwan; [3]Agricultural Biotechnology Research Center; Academia Sinica; Taipei, Taiwan; [4]Institute of Biological Chemistry; Academia Sinica; Taipei, Taiwan

Keywords: WIPI, BECN1 independent, noncanonical autophagy, recombinant VP1, macrophage migration

Abbreviations: ACTB, β-actin; ATG, autophagy-related; BMM, murine bone marrow-derived macrophage; BNL, BNL 1MEA.7R.1; C1, 1,3-dibutyl-2-thioxo-imidazolidine-4,5-dione; CHX, cycloheximide; CQ, chloroquine; DAPI, 4',6-diamidino-2-phenylindole; FBS, fetal bovine serum; HEPES, 4-(2-hydroxyethyl) piperazine-1-ethanesulfonic acid; LC3, microtubule-associated protein 1 light chain 3; MAPK1/3, mitogen-activated protein kinase 1/3 (ERK1/2); MMP, matrix metalloproteinase; PtdIns3K, class III phosphatidylinositol-3 kinase; PtdIns3P, phosphatidylinositol-3-phosphate; rVP1, recombinant capsid protein VP1; SDS, sodium dodecyl sulfate; SQSTM1, sequestosome-1/p62; UVRAG, ultraviolet irradiation resistance-associated gene; WIPI, WD repeat domain, phosphoinositide-interacting; WST, water-soluble tetrazolium; Z18, $C_{18}H_{19}CIN_2OS \cdot HCl$

The monocyte/macrophage is critical for regulating immune and antitumor responses. Recombinant capsid protein VP1 (rVP1) of foot-and-mouth disease virus induces apoptosis and inhibits migration/metastasis of cancer cells. Here, we explored the effects of rVP1 on macrophages. Our results showed that rVP1 increased LC3-related autophagosome formation via WIPI1 and WIPI2 in a BECN1-independent manner. rVP1 treatment increased macrophage migration that was attenuated by knockdown of ATG5, ATG7, WIPI1 or WIPI2 and was abolished when both WIPI1 and WIPI2 were depleted. Treatment of macrophages with rVP1 increased matrix metalloproteinase-9 (MMP9) activity and phosphorylated mitogen-activated protein kinase 1/3 (MAPK1/3), two major mediators of cell migration. Knockdown of WIPI1, WIPI2, ATG5 and ATG7 but not BECN1 attenuated the rVP1-mediated increase in MAPK1/3 phosphorylation and MMP9 activity. These results indicated that rVP1 upregulated autophagy, MAPK1/3 phosphorylation and MMP9 activity to promote macrophage migration, which was dependent on WIPI1, WIPI2, ATG5 and ATG7 but not BECN1.

Introduction

Autophagy is a cellular self-digestion process involving the formation of a double-membrane vesicle termed the autophagosome that facilitates sequestration of a variety of cargo including unwanted aggregate-prone proteins, invading microorganisms and damaged organelles.[1,2] Accumulated evidence indicates that autophagy selectively degrades many types of cargo via sequestosome-1/p62 (SQSTM1) that acts as a link between the ubiquitination and autophagy machineries.[3] In most tumor cells, defective autophagy results in SQSTM1 protein accumulation.[4]

BECN1, class III phosphatidylinositol-3 kinase (PtdIns3K), and the autophagy-related (ATG) proteins ATG5 and ATG7 all play important roles in conventional autophagy.[5,6] Canonical (BECN1-dependent) autophagy activation is usually initiated by the formation of the BECN1-PtdIns3K complex which is comprised of BECN1, PtdIns3K, PIK3R4/VPS15, UV irradiation resistance-associated gene (UVRAG) or ATG14.[5] During activation of BECN1-dependent autophagy by stimulants such as serum starvation, phosphatidylinositol-3-phosphate (PtdIns3P) is generated by enzymatic activity of the BECN1-PtdIns3K complex and recruited to the membrane for autophagosome formation.[7,8] Although BECN1 is crucial for the nucleation step of microtubule-associated protein 1 light chain 3 (LC3)-related autophagosome synthesis, increasing evidence suggests that certain noncanonical (BECN1-independent) autophagy[9] can be induced independent of BECN1 or PtdIns3K in several cell types by specific stimulants.[10-16] The antitumor phenols such as resveratrol and gossypol can induce BECN1-independent autophagy.[10-12] LC3-related autophagosome formation requires ATG5 and ATG7, whereas certain autophagosomes may result from late endosomes and the trans-Golgi without participation of ATG5, ATG7 and LC3 processing.[6]

*Correspondence to: Shu-Mei Liang and Chi-Ming Liang; Email: smyang@gate.sinica.edu.tw and cmliang@gate.sinica.edu.tw
Submitted: 02/14/12; Revised: 09/24/12; Accepted: 09/27/12
http://dx.doi.org/10.4161/auto.22379

Two PtdIns3P-binding proteins, WD repeat domain, phosphoinositide-interacting 1 and 2 (WIPI1 and WIPI2) localize to the autophagic membrane.[17,18] Both WIPI1 and WIPI2 are members of the WIPI protein family[19] and are mammalian orthologs of yeast *ATG18* which has been shown to bind PtdIns3P and localize to the autophagic membrane.[17,18,20] In BECN1-dependent autophagy of mammalian cells, the recruitment of WIPI1 to autophagic membranes and the localization of WIPI2 to early autophagosomal structures also requires PtdIns3P, which positively regulates lipidation of LC3 by conjugating LC3-I (a cytosolic form of LC3) to phosphatidylethanolamine to form LC3-II, a component of the autophagosome membrane and a well-known autophagic marker.[11,17,19] To date, it is uncertain whether both WIPI1 and WIPI2 regulate the formation of the autophagosome in BECN1-independent autophagy in mammalian cells.

Phagocytic cells migrate into the circulatory system, spread to the lymph nodes and infiltrate damaged organs. This migration potential of phagocytes is tightly associated with mammalian host defense, inflammation and tissue repair.[21-23] The monocyte/macrophage is arguably the most abundant mammalian phagocyte, critical not only for clearing microorganisms, but also for providing antitumor responses, regulating immune responses and inhibiting tumorigenesis.[24,25] Recently, Drosophila hemocytes (equivalent to mammalian macrophages) have been shown to require the induction of autophagy for cortical cytoskeleton remodeling and cell recruitment to wound sites.[26] However, the role of autophagy in mammalian monocyte/macrophage motility and migration has not yet been fully examined.

Recombinant capsid protein VP1 (rVP1) of foot-and-mouth disease virus is a potential anticancer reagent.[27] It has been found by our group to induce apoptosis, suppress growth and invasion/metastasis of a variety of human cancer cell lines.[27-30] Its effects are closely associated with inhibition of the AKT1-RAF1-MAPK1/3 signaling pathway and matrix metalloproteinases (MMPs) activity.[23-25] Since it is necessary to fully understand the effect of a potential antitumor agent not only on cancer cells but also on host immune cells, study of the effects of rVP1 on monocytes/macrophages is important.

In this study, we explored the effects of rVP1 on macrophages and found that rVP1 increased puncta formation of WIPI1 and WIPI2 in macrophages and induced autophagy in a BECN1-independent manner. Migration of macrophages, unlike that of cancer cells, was enhanced rather than inhibited by rVP1. Knockdown of WIPI1, WIPI2, ATG5 and ATG7 suppressed rVP1-mediated macrophage migration. Further studies revealed that rVP1 increased MMP9 activity and MAPK1/3 phosphorylation, which was inhibited by knockdown of WIPI1, WIPI2, ATG5 and ATG7 but not BECN1. rVP1 may thus induce BECN1-independent autophagy, MAPK1/3 phosphorylation and MMP9 activity to promote macrophage migration.

Results

rVP1 induced autophagy in macrophages. To determine the effect of rVP1 on autophagy in macrophages, we first examined LC3 puncta formation and lipidation in the murine macrophage cell line RAW264.7. LC3 puncta formation and lipidation are well-known indicators of autophagy induction.[31] Immunofluorescence microscopy showed that the pattern of fluorescence of LC3 puncta increased after treatment with rVP1 (4 μM) for 4 h in cells pretreated with or without autophagy degradation inhibitor[32] chloroquine (CQ) (**Fig. 1A**). Electron microscopy revealed that double-membrane autophagosomes were formed in RAW264.7 cells treated with rVP1 (**Fig. 1B**). Western blot of cell lysate showed that rVP1 induced LC3 lipidation as indicated by the dose-dependent increase in LC3-II (**Fig. 1C**). Chloroquine enhanced the level of rVP1-induced LC3 puncta formation and lipidation (**Fig. 1A and D**), suggesting that the mechanism of action of rVP1 was via induction rather than inhibition of LC3-II degradation. To verify that this kind of autophagic effect could be observed not only in a macrophage cell line but also in normal macrophages, murine bone marrow-derived macrophage (BMM) cells were treated with rVP1. Similar effects were observed (**Fig. 1A, C and D**) as those seen in the RAW264.7 cell line. These results suggested that rVP1 induced LC3 puncta formation and lipidation to activate autophagy in macrophages.

rVP1 induced BECN1-independent autophagy. Autophagy can be induced via BECN1-dependent and BECN1-independent pathways,[9] and serum starvation is a well-known trigger of BECN1-dependent autophagy. We thus examined whether rVP1 would induce autophagy in a BECN1-dependent manner in the same way as serum starvation. By using *Becn1* shRNA silencing, we established a BECN1 stable knockdown RAW264.7 cell line, $RAW^{sh\text{-}Becn1}$. The amount of BECN1 but not SQSTM1 was reduced in BECN1 stable knockdown cells as compared with scrambled knockdown $RAW^{sh\text{-}scrambled}$ cells (**Fig. 2A**, left panel). Although serum starvation could not induce LC3 lipidation in BECN1 knockdown cells (in the presence or absence of CQ), rVP1 enhanced LC3 lipidation regardless of whether BECN1 was knocked down or not (**Fig. 2A**, right panel). Interestingly, we found that SQSTM1 level in macrophages, unlike that reported

Figure 1 (See opposite page). rVP1 induced autophagy in macrophages. RAW 264.7 or bone marrow-derived macrophage (BMM) cells were incubated with or without 2 μM chloroquine (CQ) and then 4 μM rVP1 for 4 h as indicated. (**A**) rVP1 induced LC3 puncta formation. After treatment, cells were fixed, stained with DAPI (blue), and immunolabeled with LC3 antibody followed by Alexa Fluor 488-conjugated goat anti-rabbit IgG (green). Fluorescent images were acquired by confocal microscopy. Scale bar: 2 μm. Data represent means ± SEM of quantitative analyses of LC3 puncta per cell in at least 50 cells/experiment in three independent experiments; ****$p < 0.0001$. (**B**) rVP1 induced formation of double-membrane autophagosomes. After treatment, cells were observed with transmission electron microscopy. Data represent means ± SEM of volume fraction of autophagic compartments; **$p < 0.01$. (**C**) rVP1 increased LC3 lipidation. Cells were treated with serial concentrations of rVP1 as indicated and their lysates were subjected to immunoblot analysis using antibodies against LC3. (**D**) Lysosomal degradation inhibitor CQ enhanced rVP1-mediated LC3 lipidation. Cells were incubated with 2 μM CQ for 30 min and then 4 μM rVP1 for another 4 h, unless specified otherwise. Cell lysates were collected and analyzed by immunoblot using anti-LC3 antibodies. ACTB was used as a loading control. Blots are representative of three independent experiments.

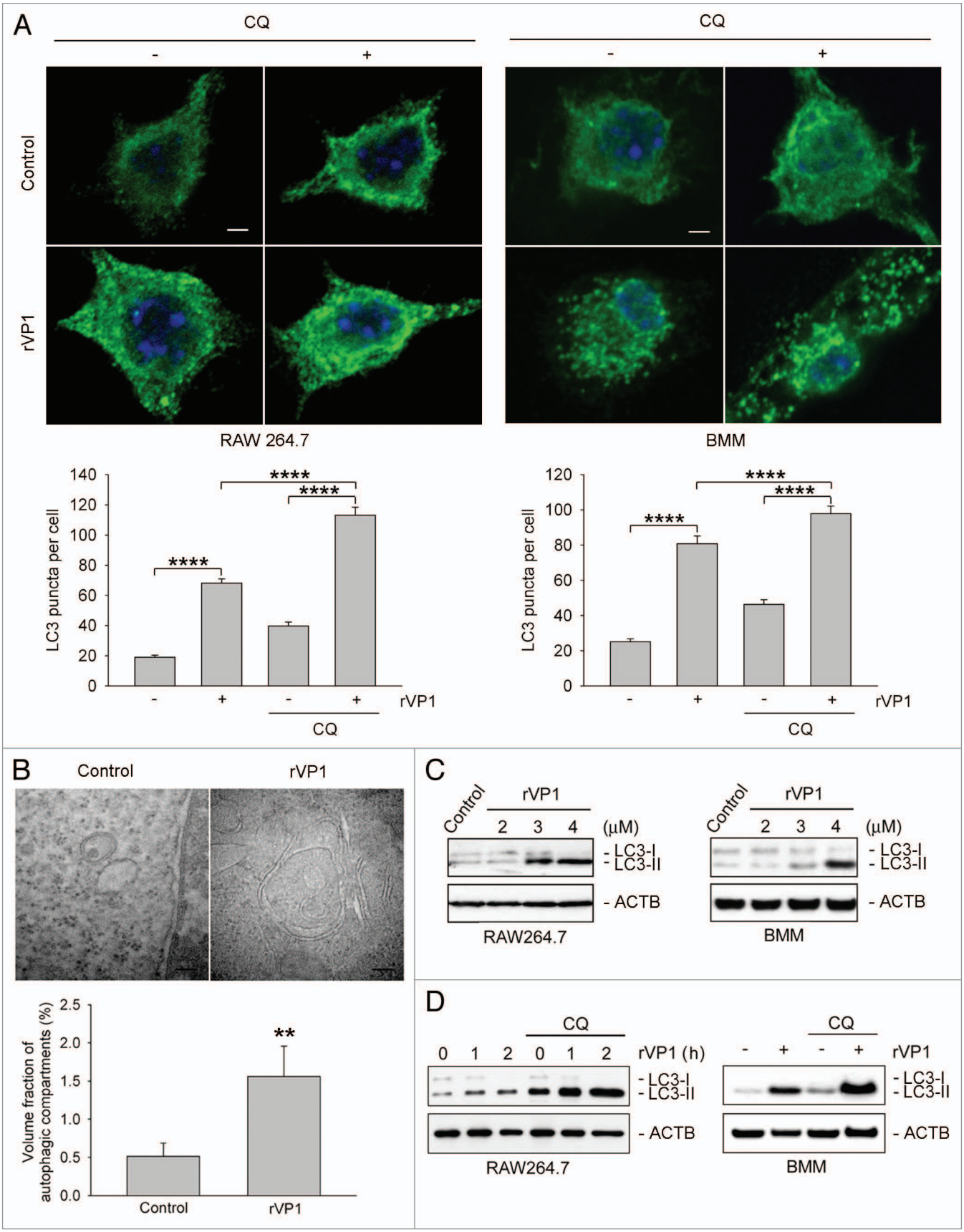

Figure 1. For figure legend, see page 6.

in cancer cells,[3,4] was not decreased by serum starvation- or rVP1-induced LC3 lipidation (**Fig. 2A**). Moreover, rVP1 increased SQSTM1 level along with LC3 lipidation in both RAW$^{sh\text{-}Becn1}$ and RAW$^{sh\text{-}scrambled}$ cells (**Fig. 2A**). Electron microscopy showed that serum starvation- but not rVP1-induced autophagosomes were decreased in RAW$^{sh\text{-}Becn1}$ cells (**Fig. 2B**). These results suggested that unlike serum starvation, rVP1 induced autophagy in a BECN1 -independent manner.

Both ATG5 and ATG7 were required for rVP1-induced autophagy. Several studies have indicated that the ATG5 and ATG7 conjugation system is required for LC3-related autophagosome and BECN1-independent autophagy.[10,12-14] To examine whether or not ATG5 and ATG7 are involved in rVP1-mediated BECN1 -independent autophagy, *Atg5* and *Atg7* were knocked down by siRNA. Our results showed that after knockdown of *Atg5* and *Atg7*, rVP1 was not able to elicit LC3 lipidation in macrophages (**Fig. 2C**), suggesting that both ATG5 and ATG7 were required for rVP1-induced BECN1-independent autophagy.

rVP1 induced WIPI1 and WIPI2 puncta formation in a BECN1-independent manner. WIPI1 and WIPI2 are mammalian orthologs of yeast *ATG18* which binds PtdIns3P and localizes to the autophagic membrane.[17] To elucidate the role of WIPI1 and WIPI2 in rVP1-mediated BECN1-independent autophagy, we examined the effects of rVP1 on WIPI1 and WIPI2 puncta formation in RAW264.7 cells. Transfection with *DsRed-Wipi1* plasmid and immunostaining with anti-WIPI2 antibodies showed that WIPI1 and WIPI2 puncta formation were increased not only after serum starvation but also with rVP1 treatment (**Fig. 3A**). These effects of rVP1 and serum starvation were enhanced by CQ treatment (**Fig. 3A**). The induction of endogenous WIPI1 and WIPI2 puncta in response to rVP1 was also observed in BMM cells (**Fig. S1**).

Knockdown of *Becn1* with siRNA in RAW264.7 cells reduced DsRed-WIPI1 puncta formation elicited by serum starvation but not that elicited by rVP1 (**Fig. 3B**, left panel). Immunostaining of WIPI2 showed that WIPI2 puncta formation was decreased in serum starvation-treated but not rVP1-treated RAW$^{sh\text{-}Becn1}$ cells (**Fig. 3B**, right panel). Collectively, these results suggested that rVP1 increased WIPI1 and WIPI2 puncta formation in a BECN1-independent manner.

WIPI1 and WIPI2 were required for autophagy mediated by rVP1. To examine whether WIPI1 is essential for rVP1-mediated BECN1-independent autophagy, RAW264.7 cells were pretreated with CQ, cotransfected with *DsRed-Wipi1* gene and *Wipi1* siRNA and then treated with rVP1. We found a significant decrease in formation of DsRed-WIPI1 puncta, and in LC3 puncta in rVP1-treated cells after the cells were transfected with *Wipi1* siRNA as compared with cells transfected with *scrambled* siRNA (**Fig. 4A**). Western blotting also showed that knockdown of WIPI1 reduced LC3 lipidation induced by rVP1 (**Fig. 4B**). These results suggested that WIPI1 was required for rVP1-mediated BECN1-independent autophagy.

To examine the role of WIPI2 in rVP1-mediated autophagy, RAW264.7 cells were pretreated with CQ, transfected with *Wipi2* siRNA and then treated with rVP1. Immunostaining of WIPI2 showed that *Wipi2* siRNA decreased the number of not only WIPI2 puncta but also LC3 puncta in rVP1-treated cells (**Fig. 4C**). Western blot results showed that knockdown of WIPI2 caused a reduction in the ratio of LC3-II/β-actin (ACTB) in rVP1 treated cells (**Fig. 4D**). These results suggested that WIPI2 was required for rVP1-induced BECN1-independent autophagy.

rVP1 increased macrophage migration via WIPI1, WIPI2, ATG5 and ATG7. Drosophila hemocytes require autophagy for cell recruitment to wound sites.[26] To examine the role of autophagy in macrophage motility, we determined trajectories of RAW264.7 cells after treatment for 22 h with serum starvation or rVP1 (4 μM) using time-lapse microscopy. The dispersive areas from the trajectories of cells treated with either serum starvation or rVP1 were significantly larger than those of cells without any treatment (**Fig. 5A**, left panel). The migration velocity of cells treated with either rVP1 or serum starvation was also faster than that of control cells (**Fig. 5A**, right panel).

Knockdown of BECN1 using *Becn1* siRNA decreased the dispersive capability and migration velocity induced by serum starvation but not that induced by rVP1 (**Fig. 5B**). Knockdown of WIPI1 or WIPI2 using their respective siRNAs reduced serum starvation-mediated dispersive capability and migration velocity. In comparison, rVP1-mediated macrophage migration was only partially abolished by knockdown of WIPI1 or WIPI2 and was abolished when both WIPI1 and WIPI2 were depleted (**Fig. 5B**). The effects of rVP1 and serum starvation were also attenuated by knockdown of ATG5 and ATG7 (**Fig. 5B**). Similar results were found by using transwell migration assays (**Fig. S2**). Taken together, these results suggested that WIPI1, WIPI2, ATG5 and ATG7 participated in the serum starvation-mediated BECN1-dependent and rVP1-mediated BECN1-independent autophagy pathway and regulated macrophage migration.

rVP1 promoted activation of MAPK1/3 and MMP9 in macrophages. We have shown recently that rVP1 inhibits cancer cell migration via inhibition of AKT1, RAF1, MAPK1/3 and matrix metalloproteinase-2 activity.[29] To examine how rVP1 increases rather than decreases macrophage migration, we determined the effect of rVP1 and serum starvation on MMP activity and phosphorylation of AKT1, RAF1 and MAPK1/3 in macrophages. Serum starvation increased phosphorylation of AKT1 and MAPK1/3 within 15 min after treatment. These effects of serum starvation reached a peak at 30 min and stayed at a level higher than the control up to at least 4 h after treatment (**Fig. 6A**). rVP1 increased phosphorylation of AKT1, RAF1 and MAPK1/3 within 15 min. Phosphorylation of AKT1 and RAF1, however, decreased very quickly and reached a level lower than the control after 30 min. Only the phosphorylation of MAPK1/3 remained higher than the control and increased dramatically at 4 h after rVP1 treatment when LC3-II level was increased (**Fig. 6B**). Interestingly, both resveratrol and gossypol, which induced WIPI1-dependent and BECN1-independent autophagy (**Figs. S3–S7**), inhibited phosphorylation of AKT1 and RAF1 (**Fig. S8A and S8B**). At 4 h after resveratrol and gossypol treatment, LC3-II level and MAPK1/3 phosphorylation in macrophages, nonetheless, increased prominently (**Fig. S8A and S8B**). Examination of MMP activity in macrophages showed that rVP1 and serum starvation increased the activity of MMP9

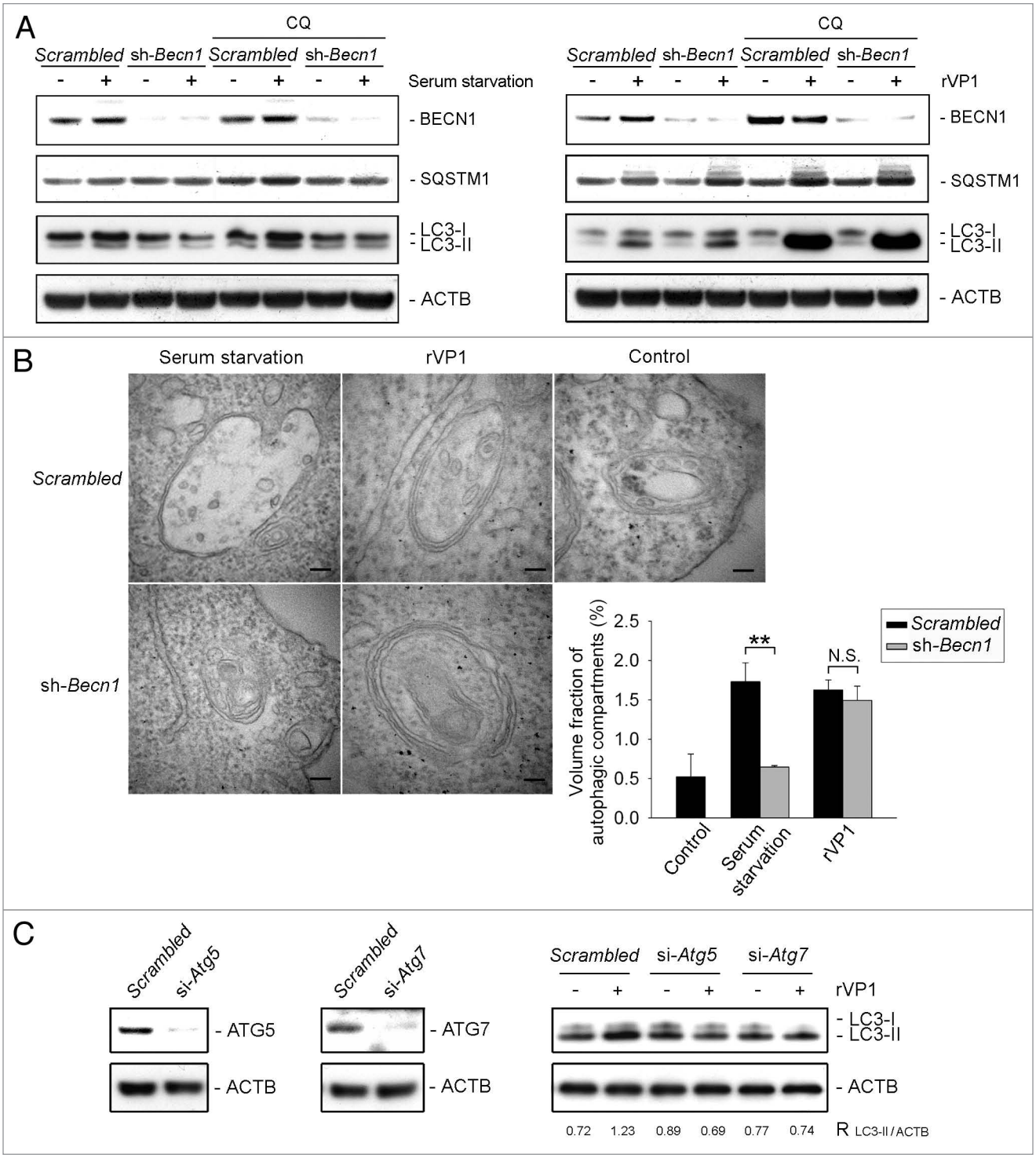

Figure 2. rVP1 induced BECN1-independent, and ATG5- and ATG7-dependent autophagy. BECN1 stable knockdown RAW264.7 cell line, RAW$^{sh\text{-}Becn\text{-}1}$, was generated by shRNA silencing as described in Materials and Methods. (**A**) Knockdown of BECN1 decreased serum starvation-mediated but not rVP1-induced LC3 lipidation. RAW264.7 cells stably knocked down with *scrambled* or *Becn1* shRNA were pretreated with or without 2 μM CQ for 30 min and then incubated with or without serum starvation for 160 min or 4 μM rVP1 for 4 h as indicated. Cells were lysed and analyzed by immunoblotting using antibodies against BECN1, SQSTM1 and LC3, respectively. ACTB was used as a loading control. (**B**) rVP1 induced formation of double-membrane autophagosomes independent of BECN1. RAW264.7 cells stably knocked down with *scrambled* or *Becn1* shRNA were serum-depleted for 160 min or incubated with 4 μM rVP1 for 4 h as indicated. After treatment, cells were collected and observed with transmission electron microscopy. Data represent means ± SEM of volume fraction of autophagic compartments; **$p < 0.01$., N.S., not significant. (**C**) rVP1 did not induce LC3 lipidation after knockdown of ATG5 and ATG7. RAW264.7 cells transfected with scrambled or siRNA of *Atg5* and *Atg7* were pretreated with 2 μM CQ and then incubated with or without 4 μM rVP1 for 4 h as indicated. Cell lysates were collected and analyzed by immunoblot using anti-LC3, anti-ATG5 and anti-ATG7 antibodies. ACTB was used as a loading control. Blots are representative of three independent experiments.

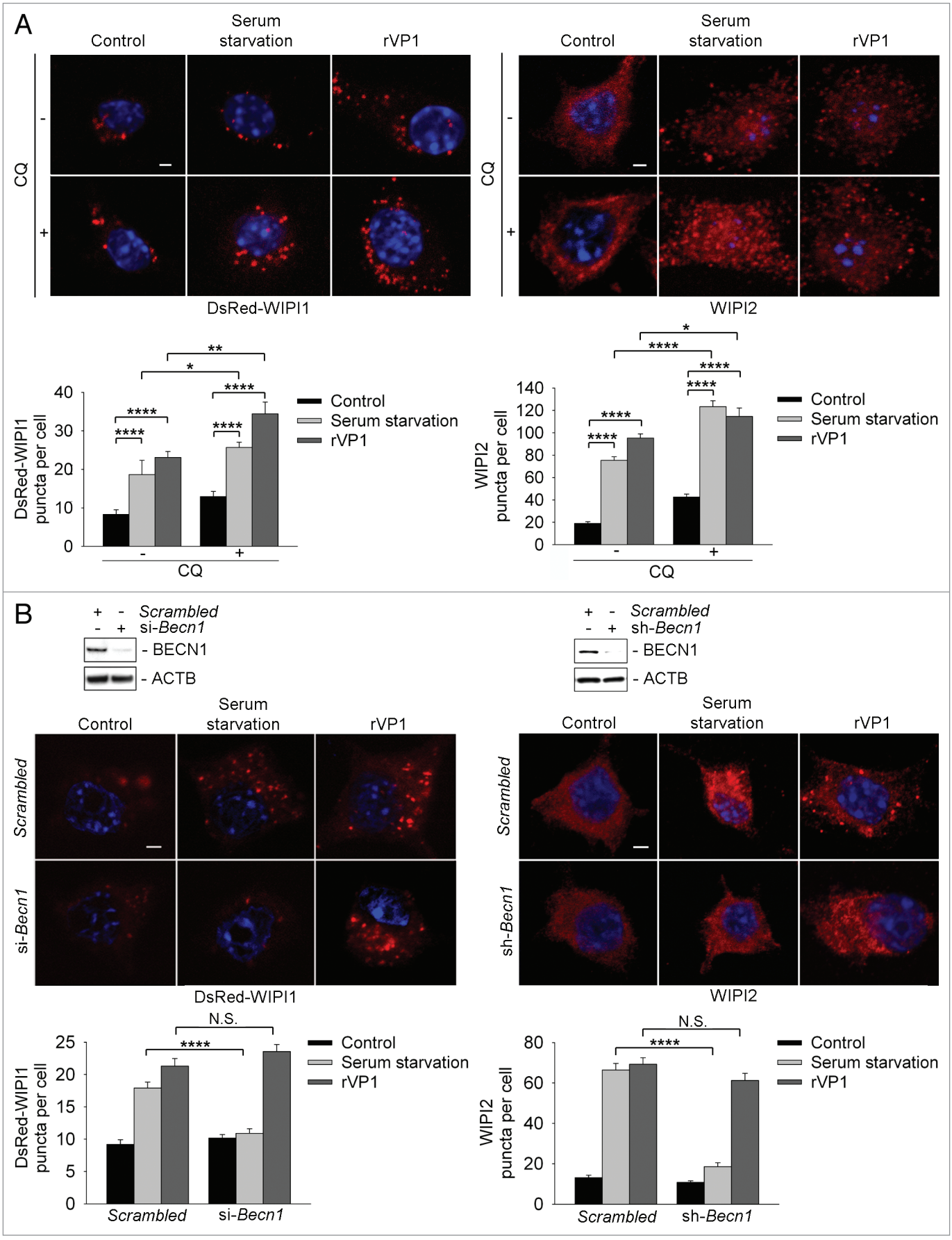

Figure 3 (See opposite page). rVP1 induced WIPI1 and WIPI2 puncta formation in a BECN1-independent manner. (**A**) rVP1 and serum starvation increased WIPI1 and WIPI2 puncta formation. To examine WIPI1 puncta formation, RAW264.7 cells were transfected with *DsRed-Wipi1* gene. The cells were then pretreated with or without 2 μM CQ for 30 min and subsequently treated with or without serum starvation for 160 min or 4 μM rVP1 for 4 h as indicated. To examine WIPI2 puncta formation, RAW264.7 cells were immunolabeled with anti-WIPI2 antibody followed by rhodamine-conjugated goat anti-mouse IgG (red). (**B**) rVP1 but not serum starvation induced DsRed-WIPI1 and WIPI2 puncta formation after knockdown of BECN1. $RAW^{sh\text{-}scrambled}$, $RAW^{sh\text{-}Becn1}$ stable cell lines or RAW264.7 cells transfected with *DsRed-Wipi1* and *scrambled* or *Becn1* siRNA were treated with serum starvation for 160 min or 4 μM rVP1 for 4 h. Fluorescent images were acquired by confocal microscopy. Scale bar: 2 μm. Data represent means ± SEM of quantitative analyses of DsRed-WIPI1 and WIPI2 puncta per cell in at least 50 cells/experiment in three independent experiments; *p < 0.05, **p < 0.01, ****p < 0.0001, N.S, not significant.

but not MMP2; whereas resveratrol, which did not increase macrophage migration (**Fig. S9A**), did not enhance the activity of either MMP9 or MMP2 (**Fig. S9B**). These results demonstrated that even though rVP1, resveratrol and gossypol all increased BECN1-independent autophagy and MAPK1/3 phosphorylation, only rVP1 was effective in promoting MMP9 activity in macrophages.

rVP1-induced MAPK1/3 phosphorylation and MMP9 activity were attenuated by knockdown of WIPI1, WIPI2, ATG5 and ATG7 but not BECN1. To examine the association between WIPI1, WIPI2, ATG5, ATG7 and rVP1-induced MAPK1/3 phosphorylation and MMP9, WIPI1, WIPI2, ATG5, ATG7 and BECN1 of RAW264.7 cells were knocked down respectively and then treated with rVP1 for 4 h. Our results showed that knockdown of WIPI1, WIPI2, ATG5 and ATG7 but not BECN1 attenuated rVP1-induced MAPK1/3 phosphorylation as compared with scrambled controls (**Fig. 7A**). Examination of MMP9 activity in conditioned media of macrophages showed that the rVP1-mediated increase in MMP9 activity was attenuated by knockdown of WIPI1, WIPI2, ATG5 and ATG7 but not BECN1 (**Fig. 7B**). Taken together these results indicated that rVP1 increased WIPI1/WIPI2-mediated LC3-related autophagy in a BECN1-independent manner, leading to enhancement in MAPK1/3 phosphorylation and MMP9 to promote migration of macrophages.

Discussion

Recently, resveratrol and gossypol and several other small molecules such as arsenic trioxide,[13] 1,3-dibutyl-2-thioxo-imidazolidine-4,5-dione (C1)[15] and $C_{18}H_{19}ClN_2OS{\cdot}HCl$ (Z18),[14] have been reported to induce BECN1-independent autophagy. In this study, we found that like resveratrol and gossypol (**Figs. S3 and S4**), rVP1 increased LC3 lipidation and autophagosome formation (**Fig. 1**) regardless of the status of BECN1 knockdown in macrophages (**Fig. 2**). These results indicated that other than small molecules, large proteins such as rVP1 can also induce BECN1-independent autophagy. Although macrophages are known to sequester toxic compounds and aggregated proteins, to the best of our knowledge, this is the first report of protein-induced BECN1-independent autophagy.

In this study, we found that rVP1 induced WIPI1 and WIPI2 puncta formation in a BECN1-independent manner (**Fig. 3**). Knockdown of WIPI1 and WIPI2 showed that both WIPI1 and WIPI2 were required for rVP1-mediated autophagy (**Fig. 4**). As resveratrol and gossypol have been reported to induce BECN1-independent autophagy in cancer cells,[10-12] we examined whether resveratrol and gossypol cause similar autophagic responses to rVP1 in macrophages. Our results showed that most of the effects of resveratrol and gossypol were similar to those of rVP1 (**Figs. S3–S5**). Knockdown of WIPI1 attenuated rVP1, resveratrol- and gossypol-induced LC3 puncta formation and lipidation (**Fig. 4**; **Fig. S6**). Our finding regarding WIPI1-dependent LC3 lipidation was consistent with that of Mauthe and his coworkers who have reported that resveratrol-mediated autophagy functionally requires WIPI1.[11] WIPI1 is thus required for rVP1-, resveratrol- and gossypol-mediated BECN1-independent autophagy.

WIPI2 is recruited to early autophagosomal structures along with ATG16L and ULK1 and is required for the formation of LC3-positive autophagosomes in HEK293A as well as HeLa, G361 and CHL-1 cancer cells.[17] Mauthe and his coworkers also have found that the effect of resveratrol on LC3-II in human G361 cells is attenuated using *siWIPI2*.[11] We found, however, that knockdown of WIPI2 decreased only rVP1 but not resveratrol- and gossypol-induced LC3 conversion in macrophages (**Fig. 4**; **Fig. S7**). Since our results showed that the effect of rVP1 was only partially blocked by knockdown of WIPI1 or WIPI2 and was abolished when both WIPI1 and WIPI2 were depleted (**Fig. 5B**), it is likely that WIPI1 and WIPI2 play distinct roles and depend on different cell types, WIPI2 may or may not be required for resveratrol- or gossypol-mediated autophagy.

Mononuclear phagocytes can transmigrate through the endothelial membrane, enter the circulation system and travel to damaged or infected organs.[23,33] Although autophagy has been reported to play a role in cell shape and spreading of macrophages,[26] the role of autophagy in macrophage migration and trafficking has not yet been evaluated. Our results showed that rVP1 enhanced macrophage migration and movement velocity which was associated with increase in MAPK1/3 phosphorylation and MMP9 activity (**Figs. 5–7**). These effects were attenuated by knockdown of WIPI1, WIPI2, ATG5 and ATG7 but not BECN1 (**Figs. 5–7**). Comparison of the effects of rVP1 with those of resveratrol and gossypol revealed that resveratrol and gossypol caused an increase in MAPK1/3 phosphorylation (**Fig. S8A and S8B**) but not MMP9 activity (**Fig. S9B**), resulting in much less increase or even a decrease in macrophage migration (**Fig. S9A**). It is thus likely that enhancement of macrophage migration by rVP1 required not only an increase in LC3-related autophagy and MAPK1/3 phosphorylation but also MMP9.

rVP1 suppresses migration/invasion and metastasis of a variety of human cancer cell lines via inhibition of the AKT1-RAF1-MAPK1/3 signaling pathway and MMP2 activity.[27-30] The results of this study, however, showed that rVP1 increased rather

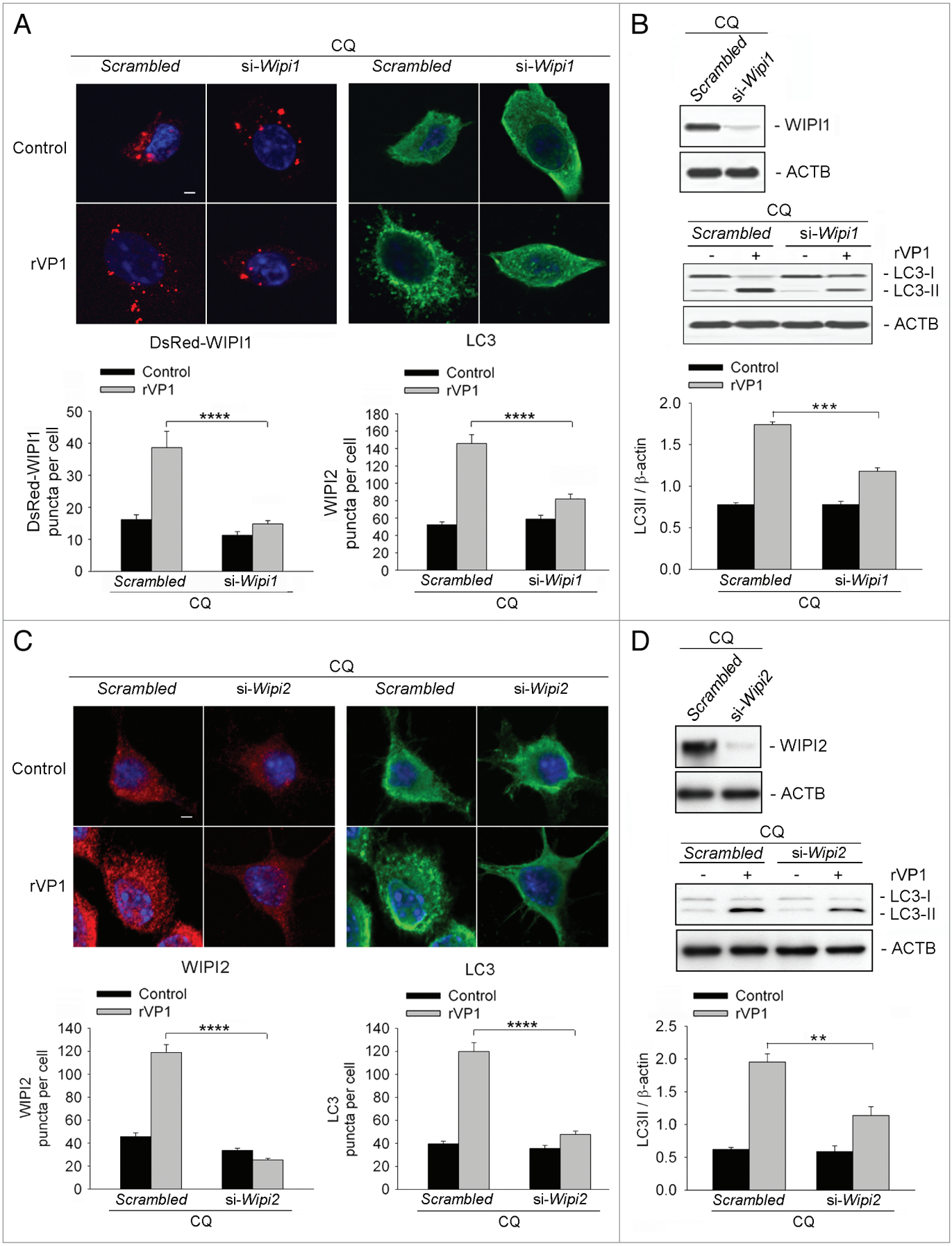

Figure 4 (See opposite page). Both WIPI1 and WIPI2 were required for autophagy mediated by rVP1. RAW264.7 cells transfected with *DsRed-Wipi1* gene and *scrambled* or *Wipi1* siRNA were pretreated with 2 μM CQ for 30 min and then incubated with or without 4 μM rVP1 for 4 h. (**A**) Knockdown of WIPI1 decreased LC3 puncta formation induced by rVP1. Cells were fixed, stained with DAPI (blue) and immunolabeled with anti-LC3 followed by Alexa Fluor 488-conjugated goat anti-rabbit IgG (green). Fluorescent images were acquired by confocal microscopy. Scale bar: 2 μm. Data represent means ± SEM of quantitative analyses of DsRed-WIPI1 and LC3 puncta per cell in at least 50 cells/experiment in three independent experiments; ****p < 0.0001. (**B**) Knockdown of WIPI1 decreased LC3 lipidation induced by rVP1. After treatment, cell lysates were collected and the expression levels of WIPI1 and LC3-II were determined by western blot analysis. ACTB was used as a loading control. Data represent the means ± SEM of densitometric measurement of LC3-II/ACTB from three independent experiments; ***p < 0.001. (**C**) Knockdown of WIPI2 decreased LC3 puncta formation in rVP1-treated cells. RAW264.7 cells transfected with *scrambled* or *Wipi2* siRNA were pretreated with 2 μM CQ for 30 min and then incubated with or without 4 μM rVP1 for 4 h and then fixed, stained with DAPI (blue) and immunolabeled with anti-WIPI2 and anti-LC3 followed by rhodamine-conjugated goat anti-mouse IgG (red) and Alexa Fluor 488-conjugated goat anti-rabbit IgG (green). Fluorescent images were acquired by confocal microscopy. Scale bar: 2 μm. Data represent means ± SEM of WIPI2 and LC3 puncta per cell in at least 50 cells/experiment in three independent experiments; ****p < 0.0001. (**D**) Knockdown of WIPI2 decreased LC3 lipidation in rVP1-treated cells. After treatment, cell lysates were collected and expression levels of WIPI2 and LC3-II were determined by western blot analysis. ACTB was used as a loading control. Data represent means ± SEM of the ratio of LC3-II/ACTB from three independent experiments; **p < 0.01.

than decreased migration of macrophages (**Fig. 5**; **Fig. S2**). This seemingly paradoxical result is not due to the induction of LC3-related autophagy as rVP1 increased LC3 lipidation in SKOV3, BNL 1MEA.7R.1 (BNL) and MCF-7 cancer cell lines (**Fig. S10**). Neither was it due to BECN1, as we also found that rVP1 increased LC3 lipidation of SKOV3 in a BECN1-independent manner (**Fig. S11**); or to WIPI1 and WIPI2, as rVP1 also induced WIPI1 and WIPI2 puncta formation in SKOV3 (**Fig. S12**). The main differences between the effects of rVP1 on cancer cells and macrophages were that rVP1 decreased MAPK1/3 phosphorylation and MMP2 activity in cancer cells,[27,28,30] whereas it increased autophagy resulting in increase of MAPK1/3 phosphorylation and MMP9 activity in macrophages (**Fig. 7**). More studies are currently underway to explore how rVP1 elicits these seemingly opposite effects on cancer cells and macrophages.

In summary, we found that rVP1 increased WIPI1/WIPI2 puncta formation and BECN1-independent autophagy in macrophages. In contrast to antitumor phenols resveratrol and gossypol, which required WIPI1 but not WIPI2, rVP1 required both WIPI1 and WIPI2 for autophagosome formation. rVP1 and serum starvation increased not only autophagy but also MAPK1/3 phosphorylation and MMP9 in macrophages to facilitate macrophage migration. These findings shed light on the induction of autophagy by rVP1, and the involvement of WIPI1 and WIPI2 in BECN1-independent autophagy and increased our understanding of the effects of rVP1-mediated BECN1-independent autophagy on MAPK1/3 phosphorylation, MMP9 activity and migration of macrophages.

Materials and Methods

Materials. rVP1 was produced as described previously.[28] Resveratrol (R5010), gossypol (G8761) and chloroquine (C6628) were purchased from Sigma Aldrich. Water-soluble tetrazolium (WST) cell viability assay kit (05015944001) were purchased from Roche. Anti-LC3 antibody (NB600-1384) was obtained from Novus. Anti-BECN1 (3738), anti-phospho AKT1 at Ser473 (9271S), anti-AKT1 (9272), anti-phospho-c-RAF1 at Ser338 (56A6), anti-phospho MAPK1/3 at Thr185/Tyr187/Thr202/Tyr204 (4370) and anti-MAPK1/3 (137F5) antibodies were all obtained from Cell Signaling Technology. Anti-WIPI1 antibody (ALX-210-955) was obtained from Enzo Life Science. Anti-WIPI2 antibody (ab101985) was obtained from Abcam. Anti-ATG5 antibody (3167-S) was obtained from Epitomics. Anti-SQSTM1/p62 antibody (H00008878-M01) was obtained from Abnova. Anti-ACTB (sc-47778), anti-RAF1 (sc-133), anti-ATG7 (sc-8668) antibodies; *scrambled* shRNA plasmid (sc-108060), *Becn1* shRNA plasmid (sc-29798-SH); and *scrambled* siRNA (sc-37007), *Becn1* siRNA (sc-29798), *BECN1* siRNA (sc-29797), *Atg5* siRNA (sc-41446), *Atg7* siRNA (sc-41448) were obtained from Santa Cruz. *Wipi1* siRNA (MSS225232) and *Wipi2* siRNA (MSS232889) were purchased from Invitrogen. RAW264.7 cell line Nucleofector Kit V (VCA-1003) was purchased from Lonza. GenMute siRNA and DNA transfection reagent (SL-100568) was obtained from SignaGen Laboratories.

Cell culture. Murine macrophage cell line RAW264.7 (TIB-71), human breast cancer cell line MCF-7 (HTB-22) and human ovarian cancer cell line SKOV3 (HTB-77) were purchased from American Tissue Culture Collection. Murine hepatocellular carcinoma cell lines BNL was kindly provided by Dr. Mi-Hua Tao, Institute of Biomedical Sciences, Academia Sinica (Taipei, Taiwan). RAW264.7, MCF-7 and BNL were maintained in DMEM medium (GIBCO, 11965-092); SKOV3 was maintained in McCoy's 5A medium (GIBCO, 16600-082) supplemented with 10% fetal bovine serum (FBS), 2 mM L-glutamine, 100 units/ml penicillin and 100 μg/ml streptomycin in a humidified 37°C incubator in a humidified atmosphere containing 5% CO_2. After reaching confluence, unless specified otherwise, cells were seeded onto wells, dishes or chamber slides for further treatments.

Isolation of bone marrow-derived macrophage cells. BMM cells were harvested from C57/B6 mice as described previously.[34] In brief, femurs and tibias were collected from mice aseptically. After removing muscles, bone marrow was exposed by cutting into the middle of bones and flushed out using syringes and needles with RPMI-1640 medium (GIBCO, 22400-089) containing 10% FBS, 20 mM HEPES, 50 μM β-mercaptoethanol, 100 units/ml penicillin and 100 μg/ml streptomycin, and filtered through a 40 μm cell strainer (BD Falcon, 352340) into a centrifuge tube. The cells were incubated with red blood cell lysis buffer for 3 min at room temperature and washed two times by RPMI-1640 medium. The cell pellet was resuspended in RPMI-1640 medium containing 10% FBS, 20 mM 4-(2-hydroxyethyl) piperazine-1-ethanesulfonic acid (HEPES), 50 μM β-mercaptoethanol, 100 units/ml penicillin,

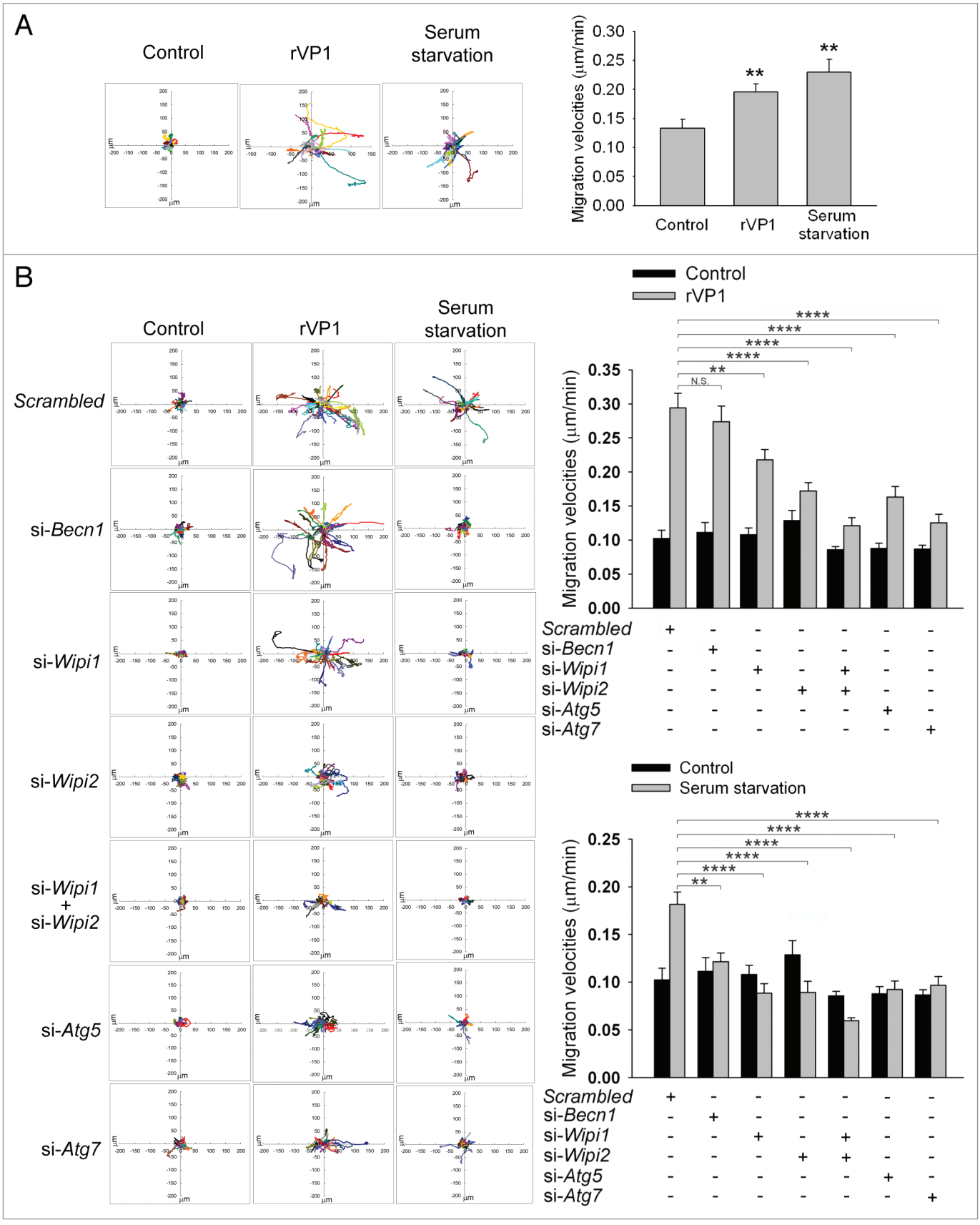

Figure 5. For figure legend, see page 15.

Figure 5 (See opposite page). rVP1 regulated macrophage migration via BECN1-independent and WIPI1/WIPI2-dependent autophagy. Trajectories of cells in response to different treatments were measured by time-lapse microscopy as described in Materials and Methods and displayed in diagrams drawn with the initial point of each trajectory placed at the origin of the plot. (**A**) rVP1 and serum starvation induced macrophage migration. Time-lapse microscopy experiments were performed to obtain serial phase-contrast images every 15 min for 22 h. Trajectories (left panel) and migration velocity (right panel) of RAW264.7 cells treated with control medium, 4 μM rVP1 or serum starvation were displayed after 22 h of time-lapse. Data represent means ± SEM of migration velocities of 20 cells with different treatments; **p < 0.01. (**B**) Knockdown of WIPI1, WIPI2, ATG5 and ATG7 but not BECN1 attenuated rVP1-induced macrophage migration. RAW264.7 cells were transfected with siRNAs of *scrambled*, *Becn1*, *Atg5*, *Atg7*, *Wipi1*, *Wipi2* and *Wipi1* plus *Wipi2* as indicated before treatment of 4 μM rVP1 or serum starvation. Trajectories and migration velocities of cells were displayed after 22 h of time-lapse. Data represent means ± SEM of migration velocity of 20 cells transfected with scrambled or target siRNA in response to rVP1 (top panel) or serum starvation (bottom panel); **p < 0.01, ****p < 0.0001, N.S., not significant.

100 μg/ml streptomycin and 20 ng/ml granulocyte macrophage colony-stimulating factor (R&D Systems, 415-ML), and seeded onto 10 cm non-tissue culture dishes in a humidified 37°C incubator in a humidified atmosphere containing 5% CO_2. Five milliliters of fresh culture medium were added to each dish every 2 d. After 6 d, the medium was removed, and the cells attached to the plates were collected and plated in tissue culture plates or chamber slides at density of 1×10^5 cells/cm^2 for rVP1 treatment. For every isolation, the cells were checked to be > 90% $CD11b^+$ and < 5% $CD25^+$ by flow cytometry.

Transmission electron microscopy. RAW264.7 macrophages treated with resveratrol, gossypol or rVP1 for 4 h were rinsed with phosphate buffered saline and harvested by TrypLE™ (Gibco, 12605-028). Cells were initially fixed by 4% paraformaldehyde containing 2.5% glutaraldehyde in 0.1 M cacodylate buffer (pH 7.3) for 30 min, embedded in 2% agarose and dissected into 1 mm cubes and further fixed overnight, then post-fixed in 1% OsO_4 in 0.1 M cacodylate buffer for 2 h. After washing with 0.1 M cacodylate buffer, cells were dehydrated in a graded series of ethanol from 30% to 100% and embedded into Spurr's resin. Resin-embedded sections were sliced into 60 nm ultrathin sections and examined with a Hitachi-H7000 transmission electron microscope (S/N 747-32-03). Quantification of autophagic compartment volume fraction in each section was conducted as described previously.[35] Random sampling was applied to each section. At least 3 squares were selected from grid squares. Multilayered autophagosomal structures with clear cytosolic components inside were point counted at 40,000× magnification and cells area were obtained at 2,000× magnification.

Immunoblot analysis. To determine LC3 lipidation and expression of BECN1, SQSTM1, WIPI1, WIPI2, ATG5 and ATG7 in cells, proteins were extracted from cell lysates using protein extraction buffer (Santa Cruz, sc-24948) containing protease inhibitors (Roche, 04906845001) and resolved in 4× sodium dodecyl sulfate (SDS) sample buffer containing 10% SDS, 0.5 μM TRIS-HCl, 4% glycerol, 1 M β-mercaptoethanol and 0.1% bromophenol blue. Protein samples were subjected to SDS-PAGE and then transferred to a polyvinylidene difluoride membrane, which was then incubated in 150 mM NaCl, 20 mM TRIS-HCl, 0.1% Tween 20 buffer containing 5% skim milk. Proteins were detected with specific primary antibodies, followed by horseradish peroxidase-conjugated secondary antibodies. Immunoreactivity was detected on Biomax ML films using Pico Chemiluminescent Substrate (Pierce, 34079) according to the manufacturer's instructions. Densitometric analyses were conducted using Image J software (Wayne Rasband, NIH) for quantitating specific immunoblot density that is normalized to ACTB.

Plasmid construction. The pDEST-*DsRed-Wipi1* and pDEST-*DsRed-WIPI1* plasmid was constructed using a Gateway recombination system (Invitrogen, 12535-029) according to the manufacturer's instructions. Briefly, *Wipi1* or *WIPI1* cDNA was amplified by PCR from the pCMV-SPORT6-*Wipi1* or pCMV-SPORT6-*WIPI1* plasmid (Open Biosystems, clone ID 5322999 for *Wipi1* and ID6055425 for *WIPI1*) respectively and subcloned into the Gateway pDONR vector to generate the pDONR-*Wipi1* and pDONR-*WIPI1* entry clone. The BioEase tag of pDEST vector (Invitrogen, 43-0111) was replaced by the red fluorescent protein (DsRed) which was amplified from the pDsRed2-Mito vector (Clontech, 632421) to generate pDEST-*DsRed* destination vector. The recombination of pDONR-*Wipi1* clone with pDEST-*DsRed* vector was facilitated by LR Clonase II Enzyme Mix (Invitrogen, 11791020) to generate pDEST-*DsRed-Wipi1* and pDEST-*DsRed-WIPI1* plasmid.

Transient transfection. The pDEST-*DeRed-Wipi1* plasmid or siRNAs of *Becn1*, *Wipi1* or *Wipi2* were transfected into RAW264.7 by Amaxa Nucleofection Cell Line Nucleofector kit V for RAW264.7 according to the manufacturer's instructions. Briefly, 5μg of plasmid or 40 nM of target siRNA was transfected to 2×10^6 RAW264.7 cells by Nucleofection Program 32 (Lonza, AAB-1001) and plated onto a 6-well plate for 24 h. For transfection in SKOV3, 20 nM of scrambled or target siRNA was transfected into 2×10^5 cells overnight by GenMute transfection reagent according to the manufacturer's instructions. The knockdown efficiency was found to be >80% by immunoblot for each target gene. Suitable concentrations of rVP1, resveratrol or gossypol in fresh culture medium were added after siRNA transfection.

Stable clone establishment. To establish stable *Becn1* silencing clones, 40 nM of *scrambled* or *Becn1* shRNA was transfected into RAW264.7 cells by Amaxa Cell Line Nucleofector Kit V at program 32 according to the manufacturer's instructions. In brief, after nucleofection for 24 h a pool of *Becn1* silencing clones were selected with 5 μg/ml puromycin. The pools of selected clones were cultured in a humidified 37°C incubator in a humidified atmosphere containing 5% CO_2 in DMEM medium containing 10% FBS, 2 mM L-glutamine, 100 units/ml penicillin, and 100 μg/ml streptomycin which was supplemented with 5 μg/ml puromycin for scrambled and *Becn1* silencing clones.

Presence and localization of rVP1 in cells. The cellular distribution of rVP1 in the membrane, cytosol and nucleus of

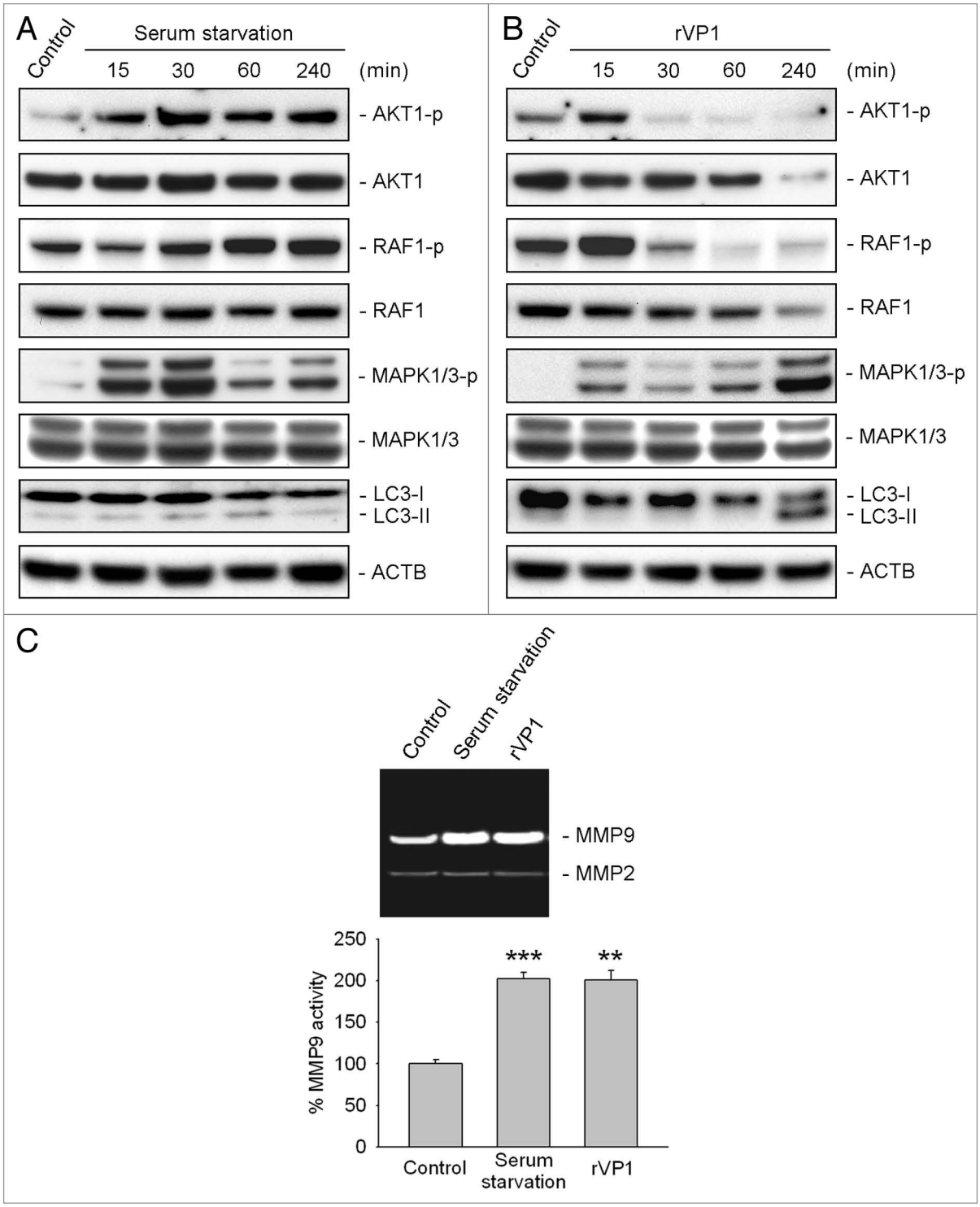

Figure 6. rVP1 increased phosphorylation of MAPK1/3 and MMP9 activity. RAW 264.7 cells were treated with serum starvation or 4 μM rVP1 for 15 to 240 min as indicated. (**A and B**) Cell lysates were collected and subjected to immunoblot analysis using antibodies against LC3, phosphorylated AKT1 at Ser473, phosphorylated RAF1 at Ser338, phosphorylated MAPK1 (Thr185/Tyr187), phosphorylated MAPK3 (Thr202/Tyr204) and their non-phosphorylation control. ACTB was used as a loading control. Blots are representative of three independent experiments. (**C**) RAW 264.7 cells were treated with serum starvation or 4 μM rVP1 for 24 h and cell conditioned media were collected. MMP activity was examined by gelatin zymographic analysis. Data represent means ± SEM of three independent experiments; $^{**}p < 0.01$, $^{***}p < 0.001$.

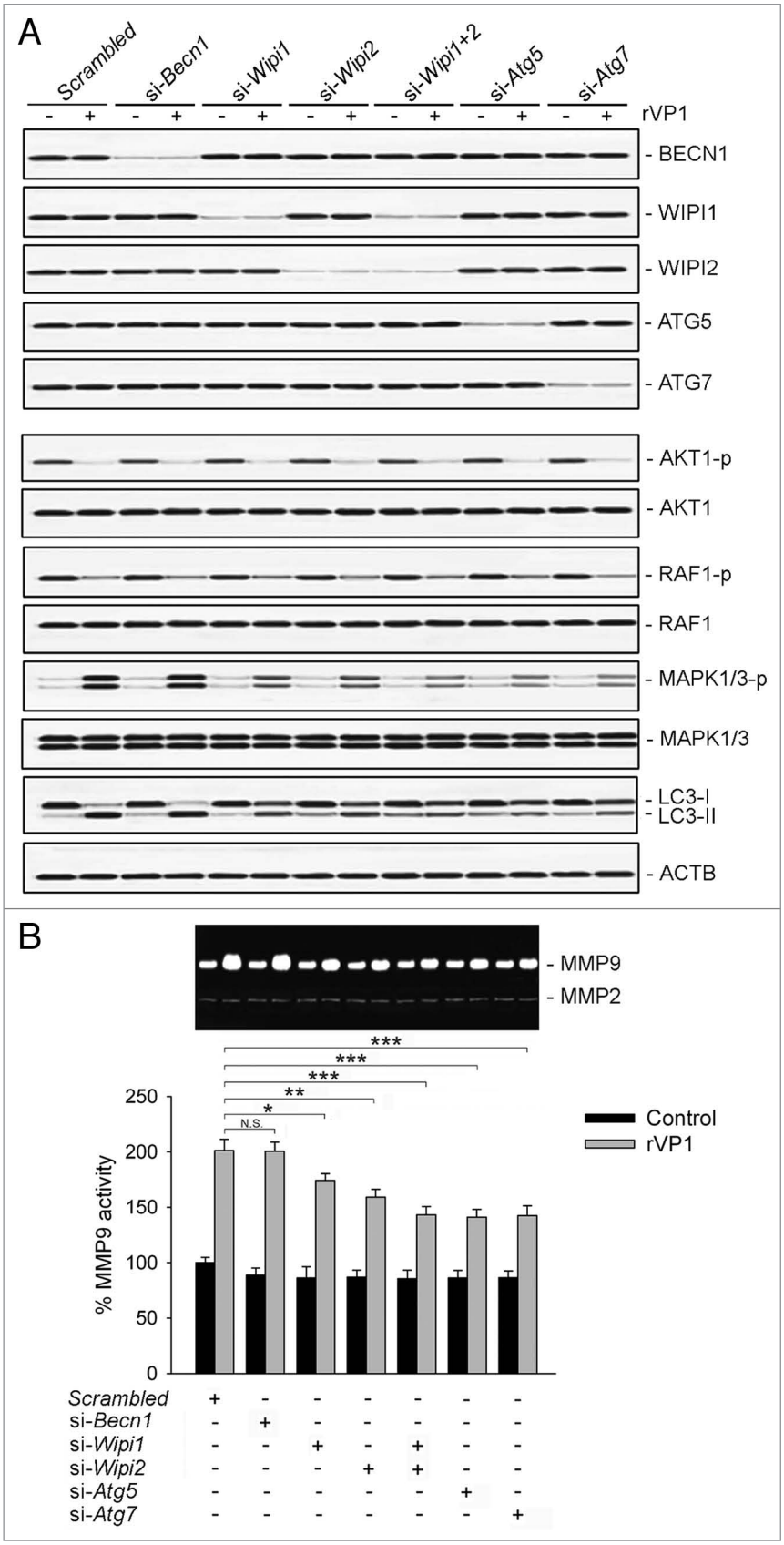

Figure 7. Knockdown of WIPI1, WIPI2, ATG5 and ATG7 but not BECN1 attenuated rVP1-mediated MAPK1/3 phosphorylation and MMP9 activity. (**A**) RAW264.7 cells transfected with *scrambled* or target siRNA as indicated were incubated with or without 4 μM rVP1 for 4 h. Cell lysates were collected and subjected to immunoblot analysis using antibodies against LC3, phosphorylated AKT1 at Ser473, phosphorylated RAF1 at Ser338, phosphorylated MAPK1 (Thr185/Tyr187), phosphorylated MAPK3 (Thr202/Tyr204) and their nonphosphorylation controls. ACTB was used as a loading control. Blots are representative of three independent experiments. (**B**) Knockdown of WIPI1, WIPI2, ATG5 and ATG7 but not BECN1 attenuated rVP1-induced MMP9 activity. Cells transfected with *scrambled* or target siRNA as indicated were incubated with or without 4 μM rVP1 for 24 h. Supernatants of cells were collected for examine MMP activity by gelatin zymographic analysis. Data represent means ± SEM of three independent experiments; *p < 0.05, **p < 0.01, ***p < 0.001, N.S., not significant.

RAW264.7 macrophages was studied at 4°C and 37°C in the presence or absence of cycloheximide (CHX) and observed by fluorescence microscopy and western blotting as shown in **Figure S13**.

Immunofluorescence staining. The formation of LC3 and WIPI2 puncta was observed by immunostaining of LC3 or WIPI2 in RAW264.7 or SKOV3 cells. Briefly, cells were seeded onto an 8-well chamber slide before treatment. After treatment, cells were fixed with 4% paraformaldehyde, followed by 0.1% Triton-X100 for 10 min and subjected to 1% BSA for 30 min at room temperature. Slides were then incubated overnight with rabbit anti-LC3 or mouse anti-WIPI2 antibodies at 4°C for 1 h at room temperature and subsequently treated with Alexa Fluor 488-conjugated goat anti-rabbit IgG (Invitrogen, A11008) or rhodamine-conjugated goat anti-mouse IgG (Invitrogen, R6393) for 30 min at room temperature. For measuring WIPI1 puncta, cells were transfected with *DsRed-Wipi1* plasmid according to the transfection procedure. Nuclei were visualized and slides were mounted by adding 4',6-diamidino-2-phenylindole (DAPI) Fluoromount G mounting buffer (SouthernBiotech, 0100-20). Images were obtained using confocal microscopy. Quantitative analyses of LC3, DsRed-WIPI1 or WIPI2 puncta per cell were undertaken by examining 50 to 100 cells in each experiment.

Cell viability assay. Cell viability in response to rVP1 was measured by WST-1 assay as described previously.[30] Briefly, 3 × 10^4 cells were seeded onto 96-well plates and

incubated at 37°C in an incubator with a humidified atmosphere containing 5% CO_2. After incubation of rVP1 for 24 h, cells were removed from the medium and 10 μL WST-1 reagent in 100 μL RPMI-1640 medium was added to each well for additional 2 h. The ratios of surviving cells were measured by ELISA reader at wavelength of 450 nm. The percentage of surviving cells was calculated as ($O.D._{treatment}/O.D._{control}$) × 100% and shown in **Figure S14**.

Cell migration assay. Cell migration assay was performed as described previously.[36] In brief, RAW264.7 cells or RAW264.7 cells transfected with siRNA of scrambled or target genes were seeded in a 35 mm dish at a density of 6×10^4 cells/cm^2. Six to eight hours after seeding or 16 h after siRNA transfection, cells were treated with 4 μM rVP1, 50 μM resveratrol or serum starvation and time-lapse microscopy experiments were performed to obtain serial phase-contrast images every 15 min for 22 h using an inverted Leica Axiovert 200 light microscope equipped with a humidified 37°C chamber in 5% CO_2. Treatment of cells with 4 μM rVP1 in medium supplemented with 10% FBS caused few, if any, cell death (**Fig. S14**). The cell trajectories and migration velocities were recorded for 22 h using the tracking point tool of Metamorph software (Molecular Devices). The average of cell migration velocities was defined as the average of 20 subsequent cell centroid displacements/one time interval between two images.

Transwell migration assay. Transwell migration assay was undertaken as described previously.[30] Briefly, transwell inserts (8 μm pore; Costar, 3422) were placed into the wells. A total of 2×10^5 cells in serum free-DMEM were placed in the upper chamber and 10% or 0.5% FBS-DMEM were added in the lower chamber. After incubation at 37°C in a humidified 5% CO_2 atmosphere for 24 h, the cells that had migrated to another side of membrane were fixed with methanol and the nonmigrated cells were mechanically removed with a cotton swab. Cells adherent on the membrane were stained with Liu's stain (ASK, 03R011/03R021). Cell numbers were examined under light microscopy at 200× magnification (Axiovert 200).

Gelatin zymographic analysis. Gelatin zymographic analysis was performed as described previously.[30] Supernatants of RAW264.7 after treatments were collected and concentrated with Vivaspin 6 centrifugal concentrators (Vivascience, VS2002). Twenty micrograms of concentrated supernatants were loaded for electrophoresis under nonreducing conditions on 10% SDS-polyacrylamide gels containing 1 mg/ml gelatin. After electrophoresis, the gels were washed in 2.5% Triton X-100 and then incubated for 20 h at 37°C in the development buffer containing 0.01 M $CaCl_2$, 0.05 M TRIS-HCl (pH 8.0). The zymographic gels were fixed in 50% methanol and 10% acetic acid and stained with 0.5% Coomassie brilliant blue R-250, then destained in 10% acetic acid. Proteolytic activity was detected as clear bands (zones of gelatin degradation) against the blue background of stained gelatin. The bands were quantified with ImageQuant 5.2 software (Amershan Bioscience).

Statistical analysis. Statistical significance and p values were determined by two-tailed t-test. LC3, DsRed-WIPI1 and WIPI2 puncta analysis is shown as the mean ± SEM from 50 to 100 cells/experiment in three independent experiments.

Disclosure of Potential Conflicts of Interest

No potential conflicts of interest were disclosed.

Acknowledgments

We thank Shu-Chen Shen (Scientific Instrument Center, Academia Sinica, Taiwan) for instruction and assistance in confocal microscope analysis; members of the electron microscope core facility, Academia Sinica, Taiwan for sample preparation and analysis; Miranda Loney (Institute of Molecular Biology and Agricultural Biotechnology Research Center Editors' Office, Academia Sinica, Taiwan) for English editorial assistance; Chiao-Li Chu for assistance in rVP1 purification; Wei-Ling Lee, Ching-Feng Chiu and Jei-Ming Peng for technical support and advice; and Academia Sinica for grant support (to S.-M.L. and C.-M.L.).

Supplemental Materials

Supplemental materials may be found here:
www.landesbioscience.com/journals/autophagy/article/22379

References

1. Levine B, Kroemer G. Autophagy in the pathogenesis of disease. Cell 2008; 132:27-42; PMID:18191218; http://dx.doi.org/10.1016/j.cell.2007.12.018
2. Maiuri MC, Zalckvar E, Kimchi A, Kroemer G. Self-eating and self-killing: crosstalk between autophagy and apoptosis. Nat Rev Mol Cell Biol 2007; 8:741-52; PMID:17717517; http://dx.doi.org/10.1038/nrm2239
3. Rusten TE, Stenmark H. p62, an autophagy hero or culprit? Nat Cell Biol 2010; 12:207-9; PMID:20190829; http://dx.doi.org/10.1038/ncb0310-207
4. Mathew R, Karp CM, Beaudoin B, Vuong N, Chen G, Chen HY, et al. Autophagy suppresses tumorigenesis through elimination of p62. Cell 2009; 137:1062-75; PMID:19524509; http://dx.doi.org/10.1016/j.cell.2009.03.048
5. Funderburk SF, Wang QJ, Yue Z. The Beclin 1-VPS34 complex--at the crossroads of autophagy and beyond. Trends Cell Biol 2010; 20:355-62; PMID:20356743; http://dx.doi.org/10.1016/j.tcb.2010.03.002
6. Nishida Y, Arakawa S, Fujitani K, Yamaguchi H, Mizuta T, Kanaseki T, et al. Discovery of Atg5/Atg7-independent alternative macroautophagy. Nature 2009; 461:654-8; PMID:19794493; http://dx.doi.org/10.1038/nature08455
7. Matsunaga K, Saitoh T, Tabata K, Omori H, Satoh T, Kurotori N, et al. Two Beclin 1-binding proteins, Atg14L and Rubicon, reciprocally regulate autophagy at different stages. Nat Cell Biol 2009; 11:385-96; PMID:19270696; http://dx.doi.org/10.1038/ncb1846
8. Sun Q, Fan W, Chen K, Ding X, Chen S, Zhong Q. Identification of Barkor as a mammalian autophagy-specific factor for Beclin 1 and class III phosphatidylinositol 3-kinase. Proc Natl Acad Sci U S A 2008; 105:19211-6; PMID:19050071; http://dx.doi.org/10.1073/pnas.0810452105
9. Scarlatti F, Maffei R, Beau I, Ghidoni R, Codogno P. Non-canonical autophagy: an exception or an underestimated form of autophagy? Autophagy 2008; 4:1083-5; PMID:18849663
10. Gao P, Bauvy C, Souquère S, Tonelli G, Liu L, Zhu Y, et al. The Bcl-2 homology domain 3 mimetic gossypol induces both Beclin 1-dependent and Beclin 1-independent cytoprotective autophagy in cancer cells. J Biol Chem 2010; 285:25570-81; PMID:20529838; http://dx.doi.org/10.1074/jbc.M110.118125
11. Mauthe M, Jacob A, Freiberger S, Hentschel K, Stierhof YD, Codogno P, et al. Resveratrol-mediated autophagy requires WIPI-1-regulated LC3 lipidation in the absence of induced phagophore formation. Autophagy 2011; 7:1448-61; PMID:22082875; http://dx.doi.org/10.4161/auto.7.12.17802
12. Scarlatti F, Maffei R, Beau I, Codogno P, Ghidoni R. Role of non-canonical Beclin 1-independent autophagy in cell death induced by resveratrol in human breast cancer cells. Cell Death Differ 2008; 15:1318-29; PMID:18421301; http://dx.doi.org/10.1038/cdd.2008.51
13. Smith DM, Patel S, Raffoul F, Haller E, Mills GB, Nanjundan M. Arsenic trioxide induces a beclin-1-independent autophagic pathway via modulation of SnoN/SkiL expression in ovarian carcinoma cells. Cell Death Differ 2010; 17:1867-81; PMID:20508647; http://dx.doi.org/10.1038/cdd.2010.53

14. Tian S, Lin J, Jun Zhou J, Wang X, Li Y, Ren X, et al. Beclin 1-independent autophagy induced by a Bcl-XL/Bcl-2 targeting compound, Z18. Autophagy 2010; 6:1032-41; PMID:20818185; http://dx.doi.org/10.4161/auto.6.8.13336
15. Wong CH, Iskandar KB, Yadav SK, Hirpara JL, Loh T, Pervaiz S. Simultaneous induction of non-canonical autophagy and apoptosis in cancer cells by ROS-dependent ERK and JNK activation. PLoS One 2010; 5:e9996; PMID:20368806; http://dx.doi.org/10.1371/journal.pone.0009996
16. Zhu JH, Horbinski C, Guo F, Watkins S, Uchiyama Y, Chu CT. Regulation of autophagy by extracellular signal-regulated protein kinases during 1-methyl-4-phenylpyridinium-induced cell death. Am J Pathol 2007; 170:75-86; PMID:17200184; http://dx.doi.org/10.2353/ajpath.2007.060524
17. Polson HE, de Lartigue J, Rigden DJ, Reedijk M, Urbé S, Clague MJ, et al. Mammalian Atg18 (WIPI2) localizes to omegasome-anchored phagophores and positively regulates LC3 lipidation. Autophagy 2010; 6:506-22; PMID:20505359; http://dx.doi.org/10.4161/auto.6.4.11863
18. Proikas-Cezanne T, Ruckerbauer S, Stierhof YD, Berg C, Nordheim A. Human WIPI-1 puncta-formation: a novel assay to assess mammalian autophagy. FEBS Lett 2007; 581:3396-404; PMID:17618624; http://dx.doi.org/10.1016/j.febslet.2007.06.040
19. Proikas-Cezanne T, Waddell S, Gaugel A, Frickey T, Lupas A, Nordheim A. WIPI-1alpha (WIPI49), a member of the novel 7-bladed WIPI protein family, is aberrantly expressed in human cancer and is linked to starvation-induced autophagy. Oncogene 2004; 23:9314-25; PMID:15602573; http://dx.doi.org/10.1038/sj.onc.1208331
20. Proikas-Cezanne T, Robenek H. Freeze-fracture replica immunolabelling reveals human WIPI-1 and WIPI-2 as membrane proteins of autophagosomes. J Cell Mol Med 2011; 15:2007-10; PMID:21564513; http://dx.doi.org/10.1111/j.1582-4934.2011.01339.x
21. Ingersoll MA, Platt AM, Potteaux S, Randolph GJ. Monocyte trafficking in acute and chronic inflammation. Trends Immunol 2011; 32:470-7; PMID:21664185; http://dx.doi.org/10.1016/j.it.2011.05.001
22. Kantari C, Pederzoli-Ribeil M, Witko-Sarsat V. The role of neutrophils and monocytes in innate immunity. Contrib Microbiol 2008; 15:118-46; PMID:18511859; http://dx.doi.org/10.1159/000136335
23. Ley K, Laudanna C, Cybulsky MI, Nourshargh S. Getting to the site of inflammation: the leukocyte adhesion cascade updated. Nat Rev Immunol 2007; 7:678-89; PMID:17717539; http://dx.doi.org/10.1038/nri2156
24. Biswas SK, Mantovani A. Macrophage plasticity and interaction with lymphocyte subsets: cancer as a paradigm. Nat Immunol 2010; 11:889-96; PMID:20856220; http://dx.doi.org/10.1038/ni.1937.
25. Murray PJ, Wynn TA. Protective and pathogenic functions of macrophage subsets. Nat Rev Immunol 2011; 11:723-37; PMID:21997792; http://dx.doi.org/10.1038/nri3073
26. Kadandale P, Stender JD, Glass CK, Kiger AA. Conserved role for autophagy in Rho1-mediated cortical remodeling and blood cell recruitment. Proc Natl Acad Sci U S A 2010; 107:10502-7; PMID:20498061; http://dx.doi.org/10.1073/pnas.0914168107
27. Peng JM, Liang SM, Liang CM. VP1 of foot-and-mouth disease virus induces apoptosis via the Akt signaling pathway. J Biol Chem 2004; 279:52168-74; PMID:15466859; http://dx.doi.org/10.1074/jbc.M403686200
28. Chen TA, Wang JL, Hung SW, Chu CL, Cheng YC, Liang SM. Recombinant VP1, an Akt inhibitor, suppresses progression of hepatocellular carcinoma by inducing apoptosis and modulation of CCL2 production. PLoS One 2011; 6:e23317; PMID:21826248; http://dx.doi.org/10.1371/journal.pone.0023317
29. Chiu CF, Ho MY, Peng JM, Hung SW, Lee WH, Liang CM, et al. Raf activation by Ras and promotion of cellular metastasis require phosphorylation of prohibitin in the raft domain of the plasma membrane. Oncogene 2012; PMID:22410782; http://dx.doi.org/10.1038/onc.2012.86
30. Peng JM, Chen YH, Hung SW, Chiu CF, Ho MY, Lee YJ, et al. Recombinant viral protein promotes apoptosis and suppresses invasion of ovarian adenocarcinoma cells by targeting α5β1 integrin to down-regulate Akt and MMP-2. Br J Pharmacol 2012; 165:479-93; PMID:21740408; http://dx.doi.org/10.1111/j.1476-5381.2011.01581.x
31. Mizushima N, Yoshimori T, Levine B. Methods in mammalian autophagy research. Cell 2010; 140:313-26; PMID:20144757; http://dx.doi.org/10.1016/j.cell.2010.01.028
32. Shintani T, Klionsky DJ. Autophagy in health and disease: a double-edged sword. Science 2004; 306:990-5; PMID:15528435; http://dx.doi.org/10.1126/science.1099993
33. Cougoule C, Le Cabec V, Poincloux R, Al Saati T, Mège JL, Tabouret G, et al. Three-dimensional migration of macrophages requires Hck for podosome organization and extracellular matrix proteolysis. Blood 2010; 115:1444-52; PMID:19897576; http://dx.doi.org/10.1182/blood-2009-04-218735
34. Via LE, Fratti RA, McFalone M, Pagan-Ramos E, Deretic D, Deretic V. Effects of cytokines on mycobacterial phagosome maturation. J Cell Sci 1998; 111:897-905; PMID:9490634
35. Ylä-Anttila P, Vihinen H, Jokitalo E, Eskelinen EL. Monitoring autophagy by electron microscopy in Mammalian cells. Methods Enzymol 2009; 452:143-64; PMID:19200881; http://dx.doi.org/10.1016/S0076-6879(08)03610-0
36. Roumes H, Leloup L, Dargelos E, Brustis JJ, Daury L, Cottin P. Calpains: markers of tumor aggressiveness? Exp Cell Res 2010; 316:1587-99; PMID:20193680; http://dx.doi.org/10.1016/j.yexcr.2010.02.017